Applied Catalysis B: Environmental 166–167 (2015) 353–365

Contents lists available at ScienceDirect

Applied Catalysis B: Environmental

journal homepage: www.elsevier.com/locate/apcatb

Full Length Article

Zeolites Y modified with palladium as effective catalysts for low-temperature methanol incineration

Magdalena Jabłońska[a], Anna Król[b], Ewa Kukulska-Zając[b], Karolina Tarach[a,*], Vladimir Girman[c], Lucjan Chmielarz[a], Kinga Góra-Marek[a,*]

[a] Faculty of Chemistry, Jagiellonian University in Kraków, Ingardena 3, 30-060 Kraków, Poland
[b] Oil and Gas Institute, Lubicz 25A, 31-503 Kraków, Poland
[c] Pavol Jozef Šafárik University in Košice, Department of Condensed Matter Physics, Park Angelinum 9, 041 54 Košice, Slovakia

ARTICLE INFO

Article history:
Received 15 July 2014
Received in revised form
20 November 2014
Accepted 24 November 2014
Available online 29 November 2014

Keywords:
Palladium
Zeolites
VOC
IR spectroscopy

ABSTRACT

Alumina, as well as zeolites HY and NaY modified with palladium (0.5–2.5 wt%) were tested in the process of methanol incineration to found an effective catalyst for the elimination of volatile organic compound (VOCs). Parent materials as well as their modifications with palladium were investigated with regards to their structural, textural and acidic/redox properties. The IR spectroscopy, X-ray diffraction, TEM, and low temperature N_2 sorption methods were employed for these purposes. This research shows that the Pd deposited on highly acidic steamed zeolite HY is considered as promising catalyst for the elimination of volatile organic compounds (VOCs). Both Pd^0 and Pd^{2+} species were found to be responsible for the oxidation process. Superior catalytic activity of 1.5%Pd/HY resulted from a synergistic effect of a high acidity of the zeolitic support and Pd species dispersion. The validity of Mars-van Krevelen pathway can be proposed as suitable for HCHO, CH_3OH and CH_4 oxidation.

1. Introduction

Volatile Organic Compounds (VOCs) have a significant negative impact on atmosphere, environment and human health [1,2]. The continuous increase of VOCs emission has forced the development of the different methods of their elimination. Among potential technologies for the abatement of VOCs emission, catalytic combustion is considered as the most efficient, simple and economic technology [3–5]. During the catalytic combustion, organics are converted into carbon dioxide and water or at least into the products less toxic than the original substances. Successful removal of VOCs depends on development of proper catalyst. Noble metal catalysts [e.g. 6, 7] and metal oxide catalysts [e.g. 8-11] are two main groups investigated in catalytic combustion of VOCs. Particularly, the Pd supported catalysts have been extensively studied, since palladium has been found to be promising for practical applications in the total combustion of VOCs due to its high activity at relatively low temperature, tolerance to moisture [e.g. 12-26] and higher resistance to thermal sintering in an oxidizing environment than platinum [16,22,27–31]. Palladium supported catalysts have been reported to be highly active for the oxidation of methane [e.g. 7, 32] and toluene [e.g. 33-36]. However, there are still a lot of doubts related to forms of palladium species catalytically active in the process of VOCs incineration [37]. The Pd^{2+} has been found to be active in hydrocarbons combustion, however the presence of Pd^0 also enhanced the activity of the catalysts by providing more active sites for VOCs dissociation [37–41]. Moreover, some authors claim that Pd^0 is the most active phase in VOCs catalytic oxidation and its stability is a vital factor for a catalyst [e.g. 42-47]. For methane oxidation the PdO phase has been generally believed to be more active than metallic Pd [48–54], while Pd–PdO mixture has been suggested to be active species for benzene oxidation [55].

The effect of palladium particle size on the catalytic VOCs incineration was reported to be highly dependent on the catalytic support and the specific reaction studied [56]. There is a general agreement that the oxidation rates increase with an increase in metal particle sizes [57–59]. The particle size and oxidation state of Pd had a great effect on the catalytic activity, and in the case of the catalyst containing noble metal of the same oxidation state (PdO/Pd^{2+} or Pd^0), the particle size possibly plays a decisive role in the catalytic activity [42]. On the other hand, several authors have not observed a strong dependence between the particle size and the catalytic activity [22,49,60]. Others [61–63] have observed that the supported palladium catalysts with higher palladium dispersion (i.e. smaller crystal size), shows higher catalytic activity.

* Corresponding authors. Tel.: +48 12 663 20 81.
E-mail addresses: karolina.tarach@gmail.com (K. Tarach), kinga.goramarek@gmail.com, gorak@chemia.uj.edu.pl (K. Góra-Marek).

http://dx.doi.org/10.1016/j.apcatb.2014.11.047
0926-3373/

Supports are an important component for the Pd-loaded catalysts as they often profoundly affect the generation of active species and catalytic performance [39,58]. Inorganic supports, such as alumina, zeolites and metal oxides have been widely studied as the catalytic supports for oxidation of VOCs [16,64–66,13]. Okumura et al. and Muto et al. [39,51,58] have reported that the acidity of the support was one of the most important factors determining the Pd dispersion. Moreover, it has been demonstrated that the Brønsted acid sites affected both dispersion and oxidation state of Pd species [51,67]. Different types of porous supports were widely used for the Pd-loaded catalysts, such as ZSM-5 (MFI) [e.g. 51, 55,68], MOR [e.g. 51], MCM-48 [e.g. 55], BEA [e.g. 69-72], and FAU [e.g. 69]. For Pd supported zeolites the combustion activity of Pd was considerably governed by the type of zeolite structure, Al concentration and kind of cation balancing of the zeolite framework charge [51].

This study was aimed to evidence the influence of the acid/base properties of different supports (HY, NaY, Al_2O_3) on dispersion and oxidation state of palladium. Consequently, the catalytic performance of the supports with various amounts of Pd deposited was evaluated in total oxidation of methanol, which was used as a model volatile organic compound.

2. Experimental

2.1. Catalyst preparation

γ-Al_2O_3 (Sasol), zeolite NaY (CBV 100, Zeolyst), and steamed zeolite HY (CBV 500, Zeolyst) were used as catalytic supports for palladium deposition. The synthesis of catalysts containing palladium was conducted basing on previously developed methods [73–75], using aqueous solution of $PdCl_2$ (2.23×10^{-3} M). The pH of solutions was kept in the range of 3–4 by addition of suitable amounts of an HCl solution (0.1 M). The molar ratio of $PdCl_2$:HCl was 1:5.

The synthesis of catalysts was conducted as follows: an appropriate (e.g. 200 mg) amount of support was added to specified volume of a $PdCl_2$ solution (e.g. 33 cm^3 to obtain 2.5 wt%), and the obtained suspension was stirred at room temperature until complete adsorption of Pd^{2+} ions. Completeness of Pd adsorption was colorimetric monitored by the reaction with thiourea. Then, the solid was filtered and washed with distilled water until Cl^- ions were absent in a filtrate. Finally, the samples were dried at room temperature. Solutions of precursor were prepared in-situ. Time necessary to complete adsorption of Pd^{2+} ions from solution was 24 h.

2.2. Characterization methods

The characterization methods presented below were applied to the samples without any treatment under air or hydrogen conditions.

2.2.1. Chemical analysis of metal content, structural and textural studies

Pd content in the samples was determined by ICP AES analysis (Table 1) using a high-performance sequential plasma spectrometer (Model ARL 3410 ICP). Palladium loading was designated at wave lengths of 360.955 and 340.458 nm. In the first step, the solid samples were digested (in a mixture of HF, HCl and HNO_3) in a microwave oven using a special temperature program. Then, aliquots of solution were diluted to volume of 100 cm^3 using deionized water. Pd content in the resulting samples varied from 0.5 to 2.5 wt%. The sample codes include the information about the Pd loading.

The BET surface area and pore volume of the samples were determined by N_2 sorption at −196 °C using a 3Flex (Micromeritics) automated gas adsorption system. Prior to the analysis, the samples were degassed under vacuum at 250 °C for 24 h. The specific surface area (S_{BET}) was determined using BET (Brunauer–Emmett–Teller) model according to Rouquerol recommendations [76]. The micropore volume and specific surface area of micropores were calculated using the Harkins-Jura model (*t*-plot analysis). All textural parameters are summarized in Table 1.

The X-ray diffraction (XRD) patterns of the samples were recorded with a D2 Phaser diffractometer (Bruker) using Cu Kα radiation (λ = 1.54060 Å, 30 kV, 10 mA).

The micrographs were obtained using transmission electron microscope (JEOL 2100F) working at 200 KV, with Field Emission Gun (FEG), EDX analysis and STEM detectors for bright and dark mode.

The X-ray photoelectron spectra (XPS) were measured on a Prevac photoelectron spectrometer equipped with a hemispherical VG SCIENTA R3000 analyser. The photoelectron spectra were measured using a monochromatized aluminium Al Kα source (*E* = 1486.6 eV) and a low-energy electron flood gun (FS40A-PS) to compensate the charge on the surface of nonconductive samples. The base pressure in the analysis chamber during the measurements was 5×10^{-9} mbar. Spectra were recorded with constant pass energy of 100 eV for the survey and for high-resolution spectra. The binding energy scale was referenced to the Au $4f_{7/2}$ peak (84.0 eV) of a clean gold. The composition and chemical surrounding of the sample surface were investigated on the basis of the areas and binding energies of Pd 3d, Al 2p, Si 2p and O 1s photoelectron peaks. The fitting of high-resolution spectra was provided through the CasaXPS software.

2.2.2. IR spectroscopy studies with probe molecules

Prior to FTIR studies, all the samples were formed into the self-supporting wafers (ca. 5 mg^{-1} cm^2) and in situ thermally treated in quartz home-made IR cell at 550 °C under high vacuum for 1 h. Quantitative experiments were carried out with the use of pyridine as a probe molecule. The measurements were realized by saturation of all acid sites in the samples with pyridine (POCh, Gliwice, Poland) at 130 °C and subsequently, physisorbed pyridine molecules were removed by evacuation at the same temperature for 20 min. The concentrations of both Brønsted and Lewis acid sites were calculated from the maximum intensities of the PyH^+ and PyL bands and corresponding values of the extinction coefficients [77] (Section 3.3.1).

Sorption of formaldehyde (Aldrich), methanol (Aldrich, 99.8%) and methane (Linde Gas, Poland, 99.5%) were performed on the vacuum pre-treated samples. Gaseous formaldehyde was produced by heating (at ca. 640 °C) of paraldehyde (Aldrich). Spectra were recorded with a Bruker Tensor 27 spectrometer equipped with an MCT detector. The spectral resolution was of 2 cm^{-1}.

All the IR spectra were normalized to the same mass of sample. The impregnation procedure did not influence the size of grains and support structure, thus the same properties of support (identical structure, the same density of T-atoms) were considered. Such normalization is equivalent to the internal standard methodology based on the same intensity of the 2100–1500 cm^{-1} overtone bands. The spectra of the Pd-modified supports normalized to the same sample mass exhibited identical intensity of the overtone bands.

2.3. Catalytic tests

Prepared materials were tested as catalysts of total methanol oxidation. The catalytic experiments were performed under atmospheric pressure in a fixed-bed flow microreactor system (i.d., 7 mm; l., 240 mm). The reactant concentrations were continuously measured using a quadruple mass spectrometer RGA 200

Table 1
Chemical analysis and textural parameters of the studied supports and their Pd modified forms. Average size of Pd particle (∅) in nm derived from TEM studies.

Samples	Pd_{ICP}/μmolg^{-1}	S_{BET}/m^2 g^{-1}	S_{micro}/m^2 g^{-1}	V_{pore}/cm^3 g^{-1}	∅/nm
Al_2O_3	0	264	–	0.39	–
0.5 wt% Pd/Al_2O_3	44	250	–	0.32	n.d.
1.0 wt% Pd/Al_2O_3	98	231	–	0.29	n.d.
1.5 wt% Pd/Al_2O_3	148	200	–	0.22	n.d.
2.5 wt% Pd/Al_2O_3	249	181	–	0.15	7–10 (70)*
					5–6 (15)
					11–13 (15)
				V_{micro}/cm^3 g^{-1}	
NaY	0	890	800	0.29	–
0.5 wt% Pd/NaY	47	800	725	0.25	n.d.
1.0 wt% Pd/NaY	95	790	719	0.21	n.d.
1.5 wt% Pd/NaY	132	650	588	0.18	3.0 (70)*
					2 (20)*
					4 (10)*
2.5 wt % Pd/NaY	280	600	510	0.13	*4.0 (50)**
					3.0 (40)*
					5.0 (10)*
HY	0	1037	942	0.36	–
0.5 wt% Pd/HY	47	937	850	0.31	n.d
1.0 wt% Pd/HY	94	926	840	0.31	n.d
1.5 wt% Pd/HY	141	865	776	0.30	2.0 (66)*
					3.0 (34)*
2.5 wt % Pd/HY	235	813	728	0.24	2.0 (75)*
					3.0 (25)*

* *x*% of the total population of Pd particles.

(PREVAC) connected directly to the reactor outlet. Prior to the catalytic test each sample of the catalyst (50 mg diluted with 50 mg of SiO_2 (POCH, BET 192 m^2 g^{-1}, particle size of 120–355 μm)) was outgassed in a flow of pure helium at constant heating rate of 10 °C min^{-1} up to 500 °C, then cooled down to room temperature. The catalyst was mixed with inactive silica in order to limit an increase in catalyst bed temperature due to exothermic methanol incineration. The isothermal saturator with a constant flow of synthetic air was used for supplying of methanol into reaction mixture. The composition of gas mixture at the reactor inlet was: [CH_3OH] = 4.0 vol.%, [O_2] = 19.0 vol.% and [N_2] = 77.0 vol.%. The reaction was studied in the range from 50 to 500 °C with the linear temperature increase of 10 °C min^{-1}. Total flow rate of the reaction mixture was 20 cm^3 min^{-1}. For the most active catalyst additional isothermal (150 °C) stability test was done using the reaction mixtures with the composition presented above. This test was run for a period of 10 h.

3. Results and discussion

3.1. Physicochemical properties of the catalysts

Supports modified with various amount of palladium were characterized with regard to their structure, texture, as well as speciation and dispersion of catalytically active metal component.

The results of XRD studies of native supports and those modified with Pd confirmed the stability of both Al_2O_3 and zeolite structures against the impregnation procedure (Fig. 1). The presence of characteristic reflections with the intensities similar to those of the native supports indicated that impregnation procedure disturbed neither the zeolite nor Al_2O_3 structure. Independently from the different Pd content (0.5–2.5 wt%) the reflections characteristic of PdO species were not identified in the diffractograms of Pd modified NaY and HY zeolites as well as of Al_2O_3. Pd-species are believed to be highly dispersed on all supports because their growth was restricted by the pore size of zeolite Y and therefore, these species have not sufficient particle size to be discriminated from the zeolite pattern [78,79].

The effect of impregnation procedure was also studied with respect to changes in textural parameters of the supports and their Pd modified forms (Table 1). The specific surface areas decreased with increasing palladium content for all materials studied. For the Pd/Al_2O_3-catalyst with the highest metal loading the specific surface area and pore volume were considerably reduced. The low dispersion of Pd species over alumina, i.e. 7–10 nm of Pd particle size, can be assigned to limited specific surface area. For the zeolite based catalysts both the drop in micropore surface and volume, especially vital for the samples with the highest Pd-loading, clearly evidenced the location of Pd-species in micropores what resulted in their plaguing. However, micropore volume was less affected by noble metal deposition in zeolite HY than NaY. Furthermore, the size of Pd-particles derived from TEM studies (Table 1) clearly confirmed that in case of strongly acidic HY support higher dispersion of noble metal clusters was achieved. Thus, a higher Brønsted acidity of HY support was beneficial to the active phase dispersion. Okumura et al. and Muto et al. [51,58] evidenced that the acidic properties of the support were one of the important factors which determine the Pd dispersion. The Pd atoms were disposed to be dispersed on the support with higher concentration of acid sites, especially with those strong acid sites that were present in steamed zeolite HY.

3.2. Catalytic activity

Zeolites and alumina modified with palladium were tested as catalysts for the process of methanol incineration. Apart from CO_2 and H_2O, no other products of methanol oxidation were detected. Fig. 2A presents results for the process performed without catalysts (empty reactor) and in the presence of pure silica used for dilution of the catalytic samples. As it can be seen the process of methanol oxidation in the gas phase is not observed at temperature below 425 °C, while conversion of CH_3OH was lower than 2% at 500 °C. While for the process performed in the presence of pure SiO_2, methanol oxidation started at 325 °C and CH_3OH was completely oxidised in the reaction stream at 500 °C. Catalytic activity of silica is possibly related to the surface defects, which could adsorb and activate methanol or/and oxygen molecules. Similar results were obtained for catalytic supports non-modified with palladium–Al_2O_3, NaY and HY (Fig 2B–D). Thus, it seems that the surface acid sites, present in these samples, do not

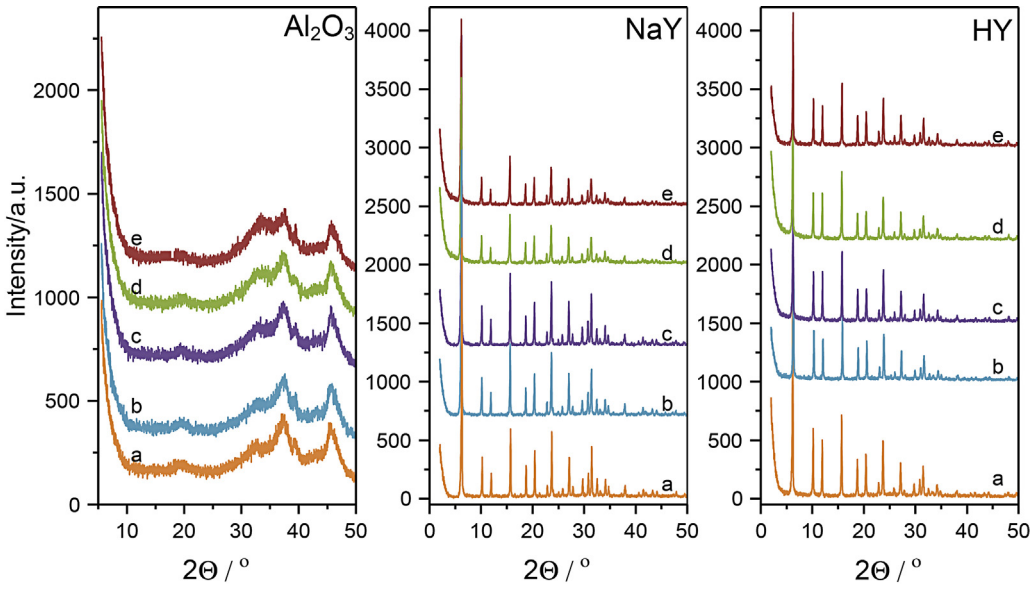

Fig. 1. XRD patterns of Al_2O_3 (A), NaY (B), and HY (C): (a) native supports, and supports modified with different Pd content 0.05 wt% Pd (b), 1.0 wt% Pd (c), 1.5 wt% Pd (d), 2.5 wt% Pd (e).

guarantee their high catalytic activity in the process of methanol oxidation.

The activity of the catalyst is frequently characterized by two parameters, T_{50} and T_{90}, which for the studied catalysts are summarized in Table 2. T_{50} refers to the temperature needed to reach 50% methanol conversion, and it is widely used to compare catalytic activity in the same reaction conditions, while T_{90} is the temperature needed to obtain 90% methanol conversion. A significant increase in the catalytic activity was observed after deposition of palladium. For the samples doped with 0.5 wt% Pd (0.5 wt%

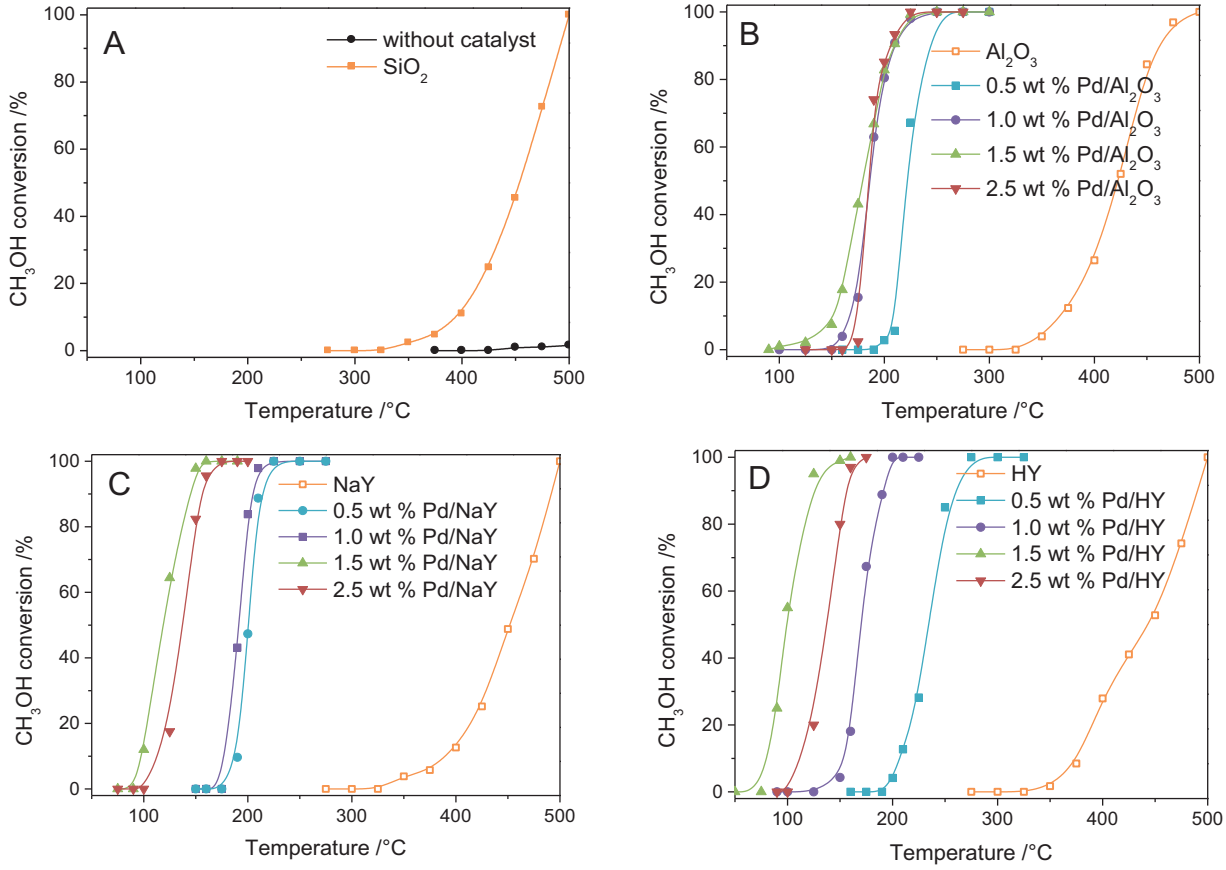

Fig. 2. Results of catalytic tests in the process of methanol incineration performed with an empty reactor and reactor containing pure SiO_2 (A) as well as over *x* wt% Pd-modified Al_2O_3 (B), NaY (C), and HY (D).

Table 2
T_{50} and T_{90} temperatures of methanol decomposition over catalysts.

Samples	T_{50}/°C	T_{90}/°C
Al_2O_3	423	462
0.5 wt% Pd/Al_2O_3	222	244
1.0 wt% Pd/Al_2O_3	186	209
1.5 wt% Pd/Al_2O_3	179	209
2.5 wt% Pd/Al_2O_3	185	206
NaY	452	492
0.5 wt% Pd/HY	201	214
1.0 wt% Pd/HY	192	205
1.5 wt% Pd/HY	119	145
2.5 wt% Pd/HY	134	157
HY	442	490
0.5 wt% Pd/HY	235	261
1.0 wt% Pd/HY	170	192
1.5 wt% Pd/HY	90	120
2.5 wt% Pd/HY	137	156

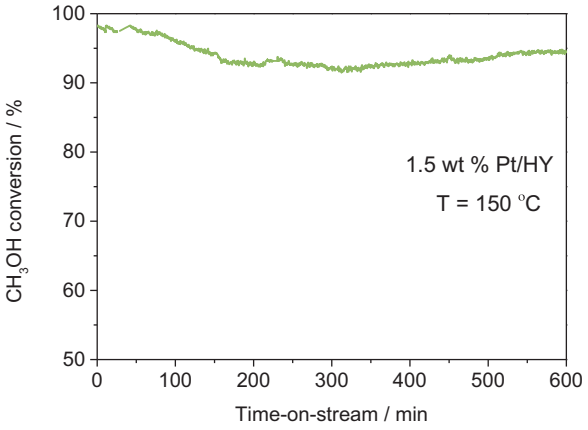

Fig. 3. Stability tests performed for the 1.5 wt% Pd/HY.

Pd/Al_2O_3, 0.5 wt% Pd/NaY, 0.5 wt% Pd/HY) oxidation of methanol starts below 200 °C, while for its complete incineration in the reaction stream temperature of 275 °C is needed. The catalysts based on HY and Al_2O_3 supports with the intended palladium content of 1.0 wt% were more active, while for the 1.0 wt% Pd/NaY catalyst no noticeable changes in activity related to the increased loading of noble metal was observed, both T_{50} and T_{90} parameters remained virtually unchanged. An increase in palladium loading to 1.5 wt% significantly more enhanced catalytic activity of the samples. For the 1.5 wt% Pd/Al_2O_3 and 1.5 wt% Pd/NaY catalysts methanol oxidation started at 125 and 100 °C, respectively. The best results were obtained for 1.5 wt% Pd/HY, which effectively converted methanol from temperature as low as 75 °C and at about 150 °C CH_3OH was completely oxidised in the reaction stream. An increase in noble metal loading to 2.5 wt% decreased activity of the HY catalysts, what is manifested by an increase in methanol conversion temperatures. This lower activity is related to the lower dispersion of active species in the 2.5 wt% Pd/HY sample as it was previously anticipated from the low-temperature nitrogen sorption and will be further evaluated in quantitative IR studies (Section 3.3.1). For the most active catalyst – 1.5 wt% Pd/HY additional long-term stability test was done. Results of these studies are presented in Fig. 3. It can be seen that during the first 150 min of the test methanol conversion dropped by about 6% and then, for the next 450 min, was nearly constant. Thus, it could be concludes that the studied catalyst presents relatively high stability under reaction conditions.

Table 3
Concentration of acid sites expressed in μmol *per* 1 gram determined in quantitative IR studies of pyridine sorption in studied materials.

Samples	$C_{Brønsted}$/μmol g^{-1}	C_{Lewis}/μmol g^{-1}	C_{Pd}/μmol g^{-1}
Al_2O_3	0	160	0
0.5 wt% Pd/Al_2O_3	0	165	5
1.0 wt% Pd/Al_2O_3	0	185	25
1.5 wt% Pd/Al_2O_3	0	210	50
2.5 wt% Pd/Al_2O_3	0	230	70
NaY	0	400	0
0.5 wt% Pd/NaY	10	430	30
1.0 wt% Pd/NaY	35	470	70
1.5 wt% Pd/NaY	55	510	110
2.5 wt% Pd/NaY	80	535	135
HY	700	350	0
0.5 wt% Pd/HY	650	390	40
1.0 wt% Pd/HY	605	440	90
1.5 wt% Pd/HY	560	485	135
2.5 wt% Pd/HY	550	500	150

3.3. IR studies

3.3.1. IR quantitative studies with pyridine as probe

In addition to specific sorption properties derived from the size and spatial arrangement of pores, the applicability of the supports was also ruled by their acidic properties. The importance of reactions undergoing with the involvement of acid sites, mainly Brønsted type, in a variety of Pd-catalysed reactions has been well documented [39,51,58]. In many cases the acidic properties were the deciding factors for the catalytic applications. Thus, the studies of the support acidity are of great importance and several methods have been developed to follow the origin and concentration of both Brønsted and Lewis acid sites. Among the methods employed for acidity characterisation, IR spectroscopy, involving the use of probe molecules, is one of the most significance. Pyridine [80] and ammonia have been used as probe molecules for the quantitative analysis of surface acidity of some solid catalysts by FTIR spectroscopy. However, the choice between these probe molecules must take into account the possible inaccessibility of metal particles to reagent molecules. Probing the palladium by carbon monoxide chemisorption revealed that Pd located in hexagonal prisms and/or sodalite cages are inaccessible to CO molecules. Only the palladium clusters in supercages are considered to be accessible to reagent molecules. The inaccessibility of metal clusters and transition metal cations to reagent molecules has been widely reported elsewhere. The interaction of methanol with Pd species has been also reported to be limited to these moieties located in supercages. Thus pyridine being able to reach the sites in supercages only, has been applied for acidity characterization of studied catalysts. It should be noted that the amount of Lewis acid sites detected with pyridine was slightly (15%) higher than with ammonia (results not presented). The most likely, a higher basicity of Py molecules allows the interaction with greater number of sites.

Interaction of pyridine with Brønsted and Lewis acid sites resulted in development of the 1450 cm^{-1} band of Py-Lewis adducts and the 1545 cm^{-1} band attributed to PyH^+ ions identifying the presence of Brønsted acid sites on the support surface. The concentrations of both Brønsted (PyH^+) and Lewis (PyL) acid sites were calculated from the maximum intensities of the PyH^+ and PyL bands and the corresponding values of the extinction coefficients: 0.61 cm μmol^{-1} and 0.11 cm μmol^{-1} for the PyH^+ and the PyL band, respectively [77].

Table 3 gathers the concentrations of the Brønsted and Lewis acid sites in the studied supports and their Pd-modified forms determined in an IR quantitative measurements of pyridine sorption. For alumina support increase of the concentration of electron-acceptor species is consistent with the amount of Pd

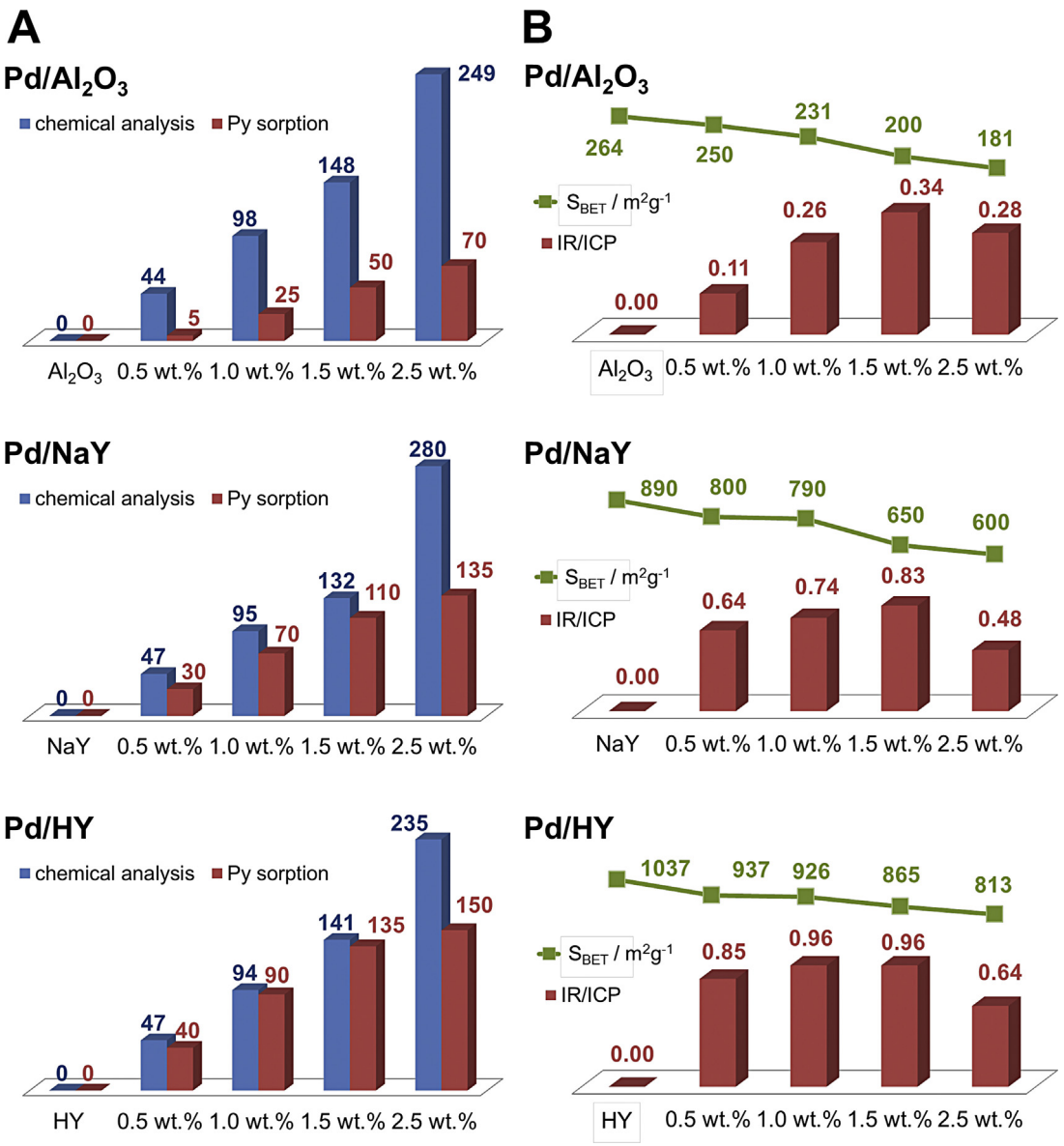

Fig. 4. (A) Comparison of the concentration of Pd centers derived from IR experiments of Py sorption and chemical analysis for native supports and those modified with different Pd content. (B) Correlation between the IR/ICP (IR: concentration of Pd species derived from Py sorption, ICP: Pd concentration from chemical analysis) ratios and surface area (S_{BET}).

impregnated. However, the amount of Lewis sites on alumina surface detected with pyridine is two-fold lower that those evidenced for the zeolitic supports. For Pd modified NaY zeolite an increase in Lewis acid centers concentration is evidenced. These electron-acceptor centers originate from palladium oxide forms. Additionally, the appearance and subsequent growth of the concentration of Brønsted acid sites is attributed to the partial Na^+/H^+ ion exchange taking place when the support was contacted with solution of Pd precursor. For HY support a decline in the amount of strongly acidic Brønsted centers (of 22%) is in line with an increase in concentration of Lewis acid centers originated from the oxide forms of palladium. Again, it can be concluded that the positively charged $Pd_xO_y^+$ species replaced the protons previously balancing the negative charge of the zeolite framework.

Concentration of surface Pd centers (in $\mu mol\,g^{-1}$) was established as the difference in the concentrations of Lewis centers in Pd-modified zeolites and native support (Table 3). Comparison of the concentrations of surface Pd centers (in $\mu mol\,g^{-1}$), determined in quantitative pyridine sorption experiments, and total Pd concentrations indicated by chemical analysis (Fig. 4), allowed calculating the contribution of Pd centers accessible for reagent molecules, thus being catalytically efficient. As mentioned earlier, for alumina support the amounts of Lewis sites detected with pyridine are two-fold lower than those evidenced for the zeolitic supports. Two factors can be decisive for the low concentration of Lewis sites detected: (i) considerably low distribution of Pd-species on alumina resulting from lower value of specific surface area in comparison to zeolites HY and NaY and/or (ii) the drop in amount of alumina electron-acceptor sites due to their partial coverage by $Pd_xO_y^+$ species.

For Pd-modified NaY a correlation between the number of Lewis acid sites generated by impregnation and total Pd content is influenced by the Na^+/H^+ ion-exchange. Some of Na^+ cations, being Lewis acid sites, were removed from the zeolite framework, in place of them Brønsted acid sites were generated, thus in consequence the number of electron-acceptor sites attributed to support was somewhat reduced. Nevertheless, the lowest dispersion of Pd-species on NaY with the increasing noble metal content is clearly

Table 4
Assignment of the IR bands appearing upon reagent adsorption (formaldehyde, methanol, and methane).

Catalyst	Band position/cm^{-1}	Assignment
HCHO gaseous	1745	—C=O
	1500	—CH_2 (scissoring)
HY	1707	C=O····H^+
Pd/HY and Pd/NaY contacted with reagents	1660	C=O····Pd^{n+}
	1640	C=O····Pd^{n+}
	1615	—COO^- antisymmetric
	1420–1350	—COO^- symmetric
	2100–2000	linear Pd^0(CO)
	1980–1970	$Pd^0{}_2(CO)_2$
		e.g. bridged $Pd^0{}_n$(CO) on (1 1 1) face
	1912–1890	bridged $Pd^0{}_n$(CO), $n > 1$
		e.g. bridged $Pd^0{}_n$(CO) on (1 0 0) face
	2348	CO_2
	1480–1450	CH_3— def.
	1630	$H_2O_{def.}$

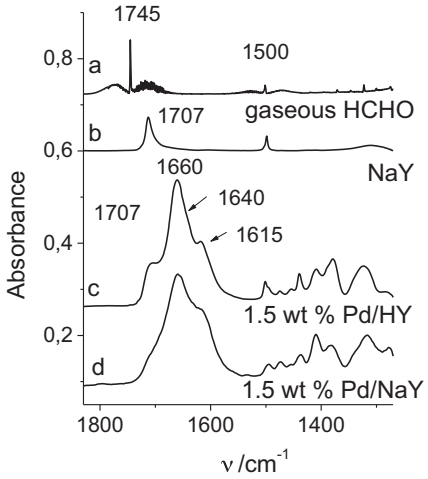

Fig. 5. IR spectra of formaldehyde gaseous (a) as well as sorbed at room temperature on zeolites HY (b), 1.5 wt% Pd/HY (c), and 1.5 wt% Pd/NaY (d).

exhibited. In the case of the Pd-catalysts based on HY support it was anticipated that impregnation of zeolite with Pd did not result in generation of other Lewis centers than those originating from Pd-forms. Thus, the differences between the concentrations of Lewis centers in Pd-modified zeolites and in native supports were attributed to various concentrations of palladium centers accessible for probe molecules. The Pd concentrations calculated from the chemical analysis and those obtained from IR measurements (Fig. 4A) are nearly identical for the catalysts with metal content in the range from 0.5 to 1.5 wt%, which clearly evidences a very high dispersion of Pd-oxide forms deposited on zeolite HY. For the 2.5 wt% Pd/HY catalyst only 64% of deposited palladium moieties was exposed on the surface pointing to a lowered dispersion of noble metal species. This result is in line with the drop of specific surface area and micropore volume, points out on micropore blocking by Pd moieties at higher noble metal loading. It is believed that those effects are responsible for lower catalytic activity of a series of the Pd/HY catalysts. The same conclusions regarding the dispersion of Pd species can be drawn from the plots of IR/ICP ratios against surface area (S_{BET}) – Fig. 4B. Consequently, for the support HY containing strong acidic sites (steamed zeolite) doped with highly dispersed palladium a synergetic effect on methanol catalytic oxidation is supposed to occur.

3.3.2. *Sorption of reagent molecules in the absence of oxygen*

Sorption of formaldehyde, methanol and methane molecules was performed on the most active zeolite-based catalysts 1.5 and 2.5 wt% Pd. The assignment of the IR bands appearing upon sorption of reagents is listed in the Table 4.

3.3.2.1. Sorption of formaldehyde. Formaldehyde (HCHO) is considered as one of the most toxic VOCs, thus its abatement is of the significant practical interests. The IR spectra of formaldehyde adsorbed in zeolites Pd/HY and Pd/NaY doped with 1.5 wt% Pd are presented in Fig. 5. Additionally, the spectrum of gaseous formaldehyde was displayed as the reference system (Fig. 5, spectrum a). The intensive band of C=O stretching vibration at 1745 cm^{-1} and the band of CH_2 scissoring vibrations at 1500 cm^{-1} are the most characteristic IR bands of the spectrum of gaseous formaldehyde (Table 4). The interaction of carbonyl group with Si(OH)Al in zeolite HY (spectrum b) was demonstrated as a red shift of C=O band to 1707 cm^{-1}. The sorption of formaldehyde on Pd-zeolites (Fig. 5, spectra c and d) also resulted in an appearance of the 1707 cm^{-1} band of formaldehyde bonded to Si(OH)Al groups. Apart from those bands originating from the interaction of formaldehyde with the zeolitic matrix, two bands at 1660 and 1640 cm^{-1} assigned to C=O interacting with two different Pd^{n+} sites of various electron acceptor properties were distinguished. The electron acceptor properties of Pd-species can be modified by the extent of neutralization of the positive Pd^{n+} charge by oxygen atoms of both the framework and those in palladium oxide clusters. Besides, an important role plays the size of noble metal clusters.

The intensities of the bands of HCHO interacting with Pd-sites (*ca.* 1660 and 1640 cm^{-1}) are of the same intensity for both Pd-modified zeolites. Thus, it can be anticipated that dispersion of Pd-species in 1.5%wt. Pd/HY and 1.5 wt% Pd/NaY materials is the same due to similar accessibility of Pd-species for HCHO molecules.

Apart from the bands of HCHO interacting with Pd^{n+} moieties (*ca.*1660 and 1640 cm^{-1}) the spectra of formaldehyde sorbed at room temperature in Pd-zeolites exhibit less intensive band at 1615 cm^{-1} as well as the complex band in the frequency region of 1425–1350 cm^{-1} (Fig. 5, spectra c and d, Table 3). The intensities of the latter bands increase with temperature up to 50 °C (Fig. 6A, spectra a and b) and it is also accompanied by the C=O. . ..Pd^{n+} band reduction. The 1615 cm^{-1} and 1420–1350 cm^{-1} bands are attributed to antisymmetric and symmetric stretching vibration of COO^- group [81]. The presence of formate ions COO^- identifies the oxidation of formaldehyde over Pd-zeolites. Prolonged contact time (30 min.) at 50 °C resulted in the consumption of formate species: the 1615 cm^{-1} band was vitally reduced, while CO adsorbed species, gaseous CO and CO_2 were also easily detected as the products of the formaldehyde oxidation (Fig. 6A). The bands at the 2100–2000 cm^{-1} frequency region are attributed to linear Pd^0(CO) carbonyls [82]. The features at 1980–1970 cm^{-1} are associated with $Pd^0{}_2(CO)_2$ adducts, whereas the band of the lowest intensity observed at 1920 cm^{-1} corresponds to CO molecules adsorbed in the bridged forms on Pd metallic species [83]. The formation of CO_2 is confirmed by the presence of the 2348 cm^{-1} band.

The facility of zeolites 1.5 wt% Pd/HY and 1.5 wt% Pd/NaY in the formaldehyde oxidation process was estimated from the relative integral intensities of the reaction products (Fig. 6B). To assure the adsorption of all reaction products on the catalyst surface the cell with reaction products was cooled down to −100 °C and then, the IR spectrum was recorded. The highest intensities of the bands of formaldehyde oxidation products, i.e. CO_2 (2348 cm^{-1}), CO in the form of Pd-carbonyls (2100–1900 cm^{-1}), and formate species (1615 cm^{-1}) was recognized for zeolite HY.

The scrutiny of the frequency of CO adsorbed on metallic Pd species delivered information on nature and dispersion of

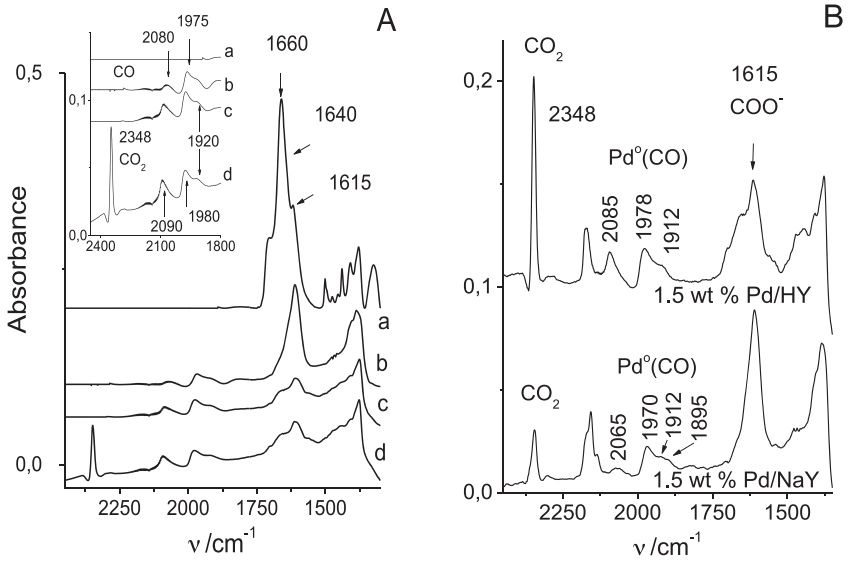

Fig. 6. (A) IR spectra of the transformation of formaldehyde over zeolite 1.5 wt% Pd/HY:
(a) spectrum of formaldehyde adsorbed at room temperature
(b) spectrum registered upon the heating of system to 50 °C
(c) spectrum registered at RT after 30 min contact time at 50 °C
(d) spectrum registered at −50 °C after 30 min contact time at 50 °C
(B) IR spectra of zeolites 1.5 wt% Pd/HY and 1.5 wt% Pd/NaY registered at −100 °C after contact with formaldehyde (50 °C for 30 min.).

Pd-clusters. The presence of the bands corresponding to CO on-top configuration (2070 cm^{-1}) and asymmetric bands attributed to isolated bridge species at lower frequencies (1900 cm^{-1}) were distinguished in 1.5 wt% Pd/HY and 1.5 wt% Pd/NaY catalysts. This result is in agreement with the presence of low coordination Pd aggregates being previously evidenced by the high dispersion found in Py-sorption measurements (Py/ICP values in Fig. 4B). The spectrum of 1.5 wt% Pd/HY presents an intense band at 2085 cm^{-1} band corresponding to linear CO adsorption, which is not present in the case of catalyst 1.5 wt% Pd/NaY. The band corresponding to linear Pd-carbonyls in 1.5 wt% Pd/NaY appeared to be less intense and shifted to a lower frequency (2065 cm^{-1}). The shift to higher frequencies of the linear band observed for Pd on HY was attributed to an less electron deficiency of Pd-species dispersed on acidic support. Similarly, the bridged Pd^0-carbonlys bands were less intense and downshifted for 1.5 wt% Pd/NaY. It has been previously reported that metal particles formed during the preparation of supported metal catalysts or formed during catalytic reaction have a structures dominated by low index planes. Energetically favoured is the formation of (1 0 0) and (1 1 1) Pd-faces. The presence of low index surfaces can be easily confirmed by CO sorption. The CO bands in the 1980–1960 cm^{-1} frequency region correspond to closed packet (1 1 1)-type Pd planes while the band at 1930–1910 cm^{-1} to open (1 0 0)-type ones [84,85]. Consequently, previous attribution of the Pd^0-carbonyls bands in the frequency region below 2000 cm^{-1} were specified in the terms of the population of (1 0 0) and (1 1 1) Pd-faces. While the (1 1 1) planes are more populated for 1.5 wt% Pd/HY, the (1 0 0) planes were more abundant for 1.5 wt% Pd/NaY.

As mentioned, formaldehyde abatement at low temperature, especially at room temperature, is an important environmental issue. The results of IR studies conformed that transformation of HCHO into carbon dioxide was achieved at temperature 50 °C, thus the Pd/HY sample meets the requirements of the commercial catalyst. In the absence of gaseous oxygen formaldehyde molecules were found to interact with oxygen-rich sites (oxide-like species PdO_x), which were alternately reduced to metallic Pd^0 forms. This observation is in line with the Mars-van Krevelen model valid for hydrocarbons oxidation over the Pd-supported catalysts.

3.3.2.2. Sorption of methanol and methane. As stated above, Pd^{n+} ions in oxo-forms dispersed in zeolite HY were found to oxidize formaldehyde to formate ions. The next step was to study the ability of Pd-species to oxidize less reactive methanol molecules. Methanol oxidation can be regarded as test case to improve the total oxidation of volatile organic compounds (VOCs). Both methanol decomposition and oxidation on noble metals are reactions which serve as models for the studies of alcohols or small organic molecules interaction with the catalysts. Thus, methanol oxidation followed by IR spectroscopy allows describing the nature of Pd-species existing on the surface of the 1.5 wt% Pd/HY and 1.5 wt% Pd/NaY catalysts.

An excess of methanol (10 Torr in the gas phase) was introduced over zeolites HY and NaY modified with 1.5 wt% Pd, at room temperature. Next IR cell was heated to 100 °C for 10 min, then cooled down to room temperature and finally the spectra were collected. The bands of methanol oxidation products can be clearly distinguished (Fig. 7A, Table 3). The weak 1660 cm^{-1} band is attributed to formaldehyde adsorbed on Pd-species. The set of bands of a negligible intensity in the region of 1480–1450 cm^{-1} originates from the vibrations of CH_3 group in non-reacted methanol. Similarly as for formaldehyde oxidation, carbon monoxide (both in the gas phase and in forms of Pd-carbonyls) and carbon dioxide (the 2348 cm^{-1} band) are also found as the products of methanol reaction with palladium moieties deposited in zeolite HY. The bands at 1630 cm^{-1} are attributed to water molecules, possibly formed either as a product of formaldehyde oxidation, being an intermediate product of methanol oxidation or methanol dehydrogenation (catalysed by protonic acid sites of the zeolitic support). Activity of 1.5 wt% Pd/HY and 1.5 wt% Pd/NaY zeolites in the methanol oxidation process was estimated from the relative integral intensities of the bands characteristics of the reaction products (Fig. 6B, spectra b and d). Again, a higher activity of the HY zeolite support over NaY was manifested.

It should be noted that sorption of methanol was carried out in the absence of oxygen. Thus, the formation of carbon dioxide evidences the presence of oxide-like Pd-species undergoing reduction while contacted with methanol. To support the role of palladium oxide species, interaction of methanol with the reoxidized

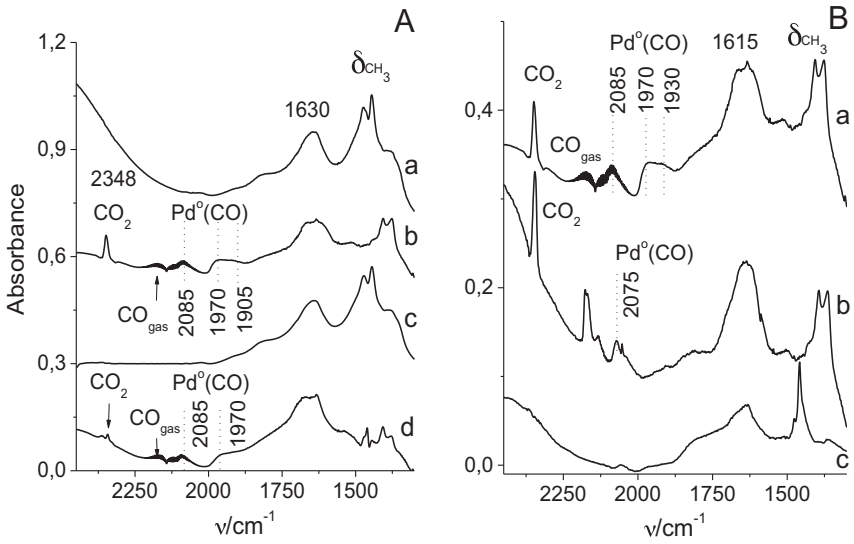

Fig. 7. (A) IR spectra recorded after sorption of methanol (10 Torr in the gas phase) in zeolites 1 5 wt% Pd/HY (a) and 1.5 wt% Pd/NaY (c) at room temperature. Spectra b and d were recorded at −50 °C after the contact of methanol (at 100 °C for 10 min) with zeolites 1.5%Pd/HY and 1.5%Pd/NaY, respectively. (B) IR spectra recorded at room temperature after sorption of methanol in the zeolite 1.5 wt% Pd/HY: (a) – without any pre-treatment, (b) – treated with O_2 at 300 °C for 30 min.,(c) – previously reduced with methanol at 100 °C for 15 min.

sample (treatment with O_2 at 300 °C for 30 min.) was performed. Only upon such treatment the spontaneous transformation of methanol into oxygenates (Fig. 6B, spectrum b) was verified. Methanol decomposition is a reaction which proceeds on metallic Pd *via* dehydrogenation to CO and hydrogen or via C—O bond scission to carbonaceous species (CH_x), CH_4 and water. These intermediate species of methanol decomposition can not only act as poison but also be involved in driving the selectivity for methanol oxidation. Thus, methanol oxidation followed by IR spectroscopy was performed on the catalyst reduced by the contact with methanol at 100 °C. The reduced catalyst with exposed metallic Pd species did not deliver further activity in methanol incineration (Fig. 7B, spectrum c). In the absence of oxygen CO, HCHO, (CHO) and CH_x species were not identified on the catalyst surface. Thus, it is clearly evidenced that the Pd-moieties, active in oxidation of HCHO and CH_3OH to carbon dioxide, can be relatively easy oxidized to oxide form by O_2, which in the next step can be reduced to metallic form by organic molecules. Therefore, the Pd-oxide moieties play a role of red-ox centres active in methanol oxidation.

Similar experimental conditions elaborated for formaldehyde and methanol oxidation were also adapted for methane oxidation (Fig. 8, Table 3). The excess of methane (10 Torr in the gas phase) was contacted with Pd-zeolites at 150 °C. After 10 min of contact time the IR cell was cooled down and then the spectra were recorded (spectrum b). An appearance of formate species (1615 cm^{-1}), carbon monoxide in both the gas phase and the adsorbed on Pd^0 species, and carbon dioxide (2348 cm^{-1}) confirms the oxidation of methane over Pd-zeolites. However, the oxidation of all methane molecules was not achieved, what is manifested by the presence of the vibration–oscillation spectrum of methane after reaction (spectrum b). Similarly as for formaldehyde and methanol oxidation, the comparison of the intensities of the bands characteristic of the reaction's products formed on the catalysts based on different zeolitic supports (HY vs. NaY) clearly shows high activity of zeolite 1.5 wt% Pd/HY in methane oxidation (spectra b and c). The CO_2 formation on 1.5 wt% Pd/HY via a complete oxidation reaction, i.e. $CH_4 + 2O_2 \rightarrow 2H_2O + CO_2$, involves weakly bonded lattice oxygen in PdO_x moieties that can be easily transferred to hydrocarbon. Such oxygen enriched palladium species in 1.5 wt% Pd/HY are responsible for the formation of a significant amount of carbon dioxide produced in the absence of gaseous oxygen.

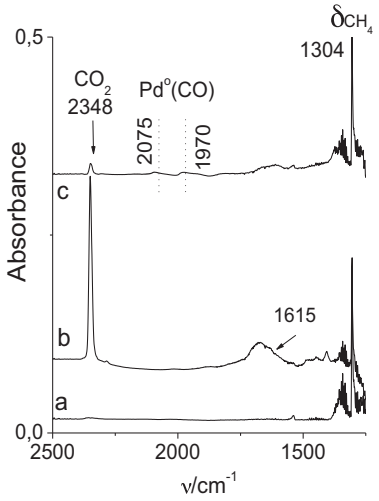

Fig. 8. IR spectrum recorded after sorption of methane (10 Torr in the gas phase) on zeolite 1.5 wt% Pd/HY at room temperature(a). Spectra b and c were recorded at −50 °C after the contact of methane (at 150 °C for 10 min) with zeolites 1.5 wt% Pd/HY and 1.5 wt% Pd/NaY, respectively.

Apart from acidity of the zeolitic supports that influenced the size and the electron properties of Pd metal clusters also acid Brønsted centres of the zeolite framework can play an important role in the catalytic process being additional reservoir of the substrate in chemisorbed form. Thus, the predominant role of protonic form of zeolite Y over sodium form in formaldehyde oxidation is postulated. The role of acid-base properties of the support in Pd-species activity has been widely discussed in the literature. Both dispersion and oxidation state of Pd were found to be sensitive to the structure type and the composition of the supports. XPS and kinetic studies revealed that the affinity for oxygen of Pd surface was associated with the acid–base character of oxides (e.g. MgO, SiO_2, Al_2O_3). Similarly, for zeolite supports the activity of Pd species was considerably dependent on the type of zeolite structure and the concentration of acid sites [67]. The Brønsted acid sites were recognized as being responsible for the generation of highly dispersed Pd species, which were active for the selective reduction

Table 5
XPS binding energy peak positions in zeolites HY and NaY of 1.5 wt% Pd content.

Peak	Binding energy [eV]	
	1.5 wt% Pd/HY	1.5 wt% PdNaY
Pd^0 $3d_{3/2}$	340.3	339.4
Pd^0 $3d_{5/2}$	335.0	334.1
Pd^{2+} $3d_{3/2}$	341.7	340.7
Pd^{2+} $3d_{5/2}$	336.4	335.5

of NO by methane in the presence of O_2 [86]. Hicks et al. [87] reported that methane combustion activity of dispersed PdO on HMFI was noticeably (up to 100 times) lower than that of the small palladium crystallites. It has been evidenced that the size effect of PdO was regulated though the degree of interaction between PdO and acid sites of HMFI [67]. What is more, Pd supported on Na-form MFI exhibited poorer durability to CH_4 combustion reaction than Pd on HMFI zeolite. The speciation of palladium in Pd/H-MOR was also found to be considerably dependent on the Al concentration of HMOR [51]. The acid–base properties regulate Pd speciation through the electronic interaction between support and Pd moieties. However, the higher specific surface area of HY in comparison to NaY support can be taken into account as an additional factor determining the dispersion of Pd-moieties. Numerous studies have been devoted to clarify the rate enhancement on acidic supports [e.g. 51, 58, 88]. Sachtler et al. [89] have suggested that Pd species in protonic zeolite Y can be considered as Pd_n-H^+ adducts, where the proton charge is delocalised over Pd-clusters. Other explanation was addressed to the polarization of small metal clusters by neighbouring cations [90]. This idea concerning electron-deficient metal atoms, which are in the vicinity of cations, has been also confirmed by quantum chemical calculation.

3.4. XPS studies

The problem of different catalytic behaviour of Pd species dispersed on zeolites HY and NaY has been followed by X-ray photoelectron spectroscopy. The Si 2p, Al 2p, O 1s peaks of the HY and NaY supports have been characterised by the same binding energy and intensity ratios for all the studied catalysts and they were identical to the data of the bare (non-modified) zeolite HY and NaY.

The XPS spectra of Pd-zeolites HY and NaY show the Pd 3d peaks (Fig. 9). The measured binding energies are presented in Table 5. The peaks attributed to Pd^{2+} $3d_{3/2}$ and Pd^{2+} $3d_{5/2}$ fit well with PdO, while the larger peaks of lower binding energies correspond to pure metallic Pd (Pd^0 $3d_{3/2}$ and Pd^0 $3d_{5/2}$). The doublet at 338.5–339.0 eV (Pd $3d_{5/2}$) and 344.5–345.0 eV (Pd $3d_{3/2}$) (Fig. 9, dotted lines) can be assigned to a satellite line accompanying electron ionization from the Pd 3d level of palladium atoms in PdO particles. This conclusion is based on an analysis of both published spectroscopic data and the experimental spectra of Pd metal and oxidized Pd foil, which exhibited satellite lines along with photolines [91,92]. Alternatively, these lines can correspond to Pd oxide species, with a high oxidation state close to 4+ (PdO_2) [93].

The values of binding energies evidences a shift for both $Pd^0{}_{3d}$ (1.0–1.1 eV) and $Pd^{2+}{}_{3d}$ (0.6–0.7 eV) when the support changes from acidic (HY) to more neutral (NaY)–Table 5. The change of the binding energy, the most probably, results from the interaction of the metal species with the support. The palladium moieties appear to be electron deficient in zeolite 1.5 wt% Pd/HY, while in 1.5 wt% Pd/NaY they are electron enriched. Consequently, the acidic nature of zeolite HY allowed the oxidation rate enhancement and therefore zeolite 1.5 wt% Pd/HY was found as the most effective catalyst.

The value of binding energy has been also found to be metal particle size dependent [94]. However, in our study the changes

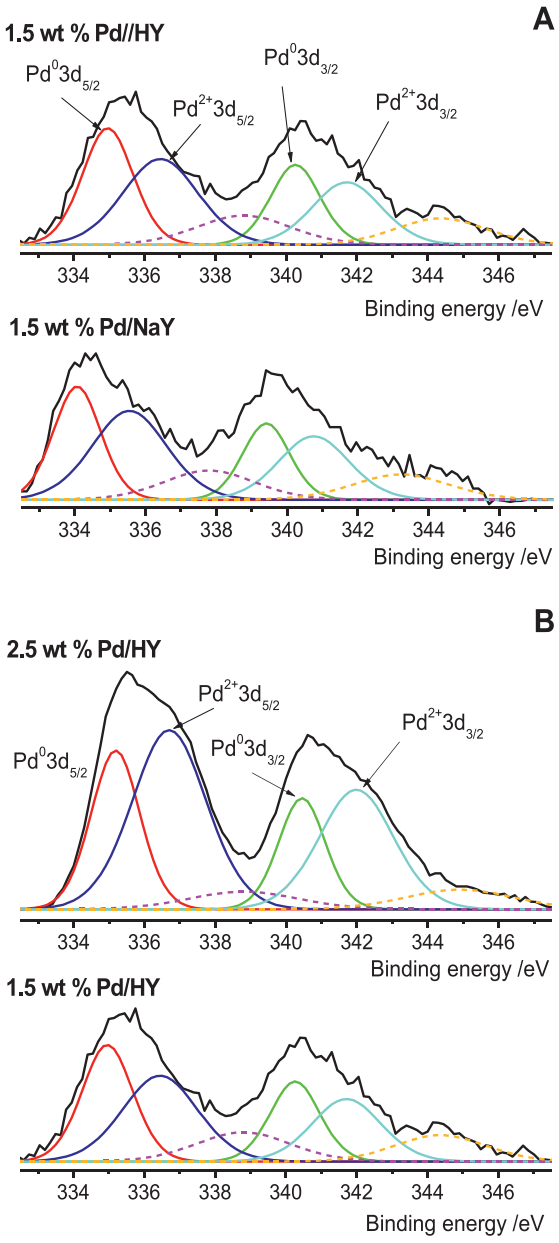

Fig. 9. XPS spectra of zeolites (A) 1.5 wt% Pd/HY and 1.5 wt% Pd/NaY, as well as (B) 2.5 wt% Pd/HY and 1.5 wt% Pd/HY.

Table 6
XPS binding energy peak positions in zeolites HY of 1.5 and 2.5 wt% Pd content.

Peak	Binding energy [eV]	
	2.5 wt% Pd/HY	1.5 wt% Pd/HY
Pd^0 $3d_{3/2}$	340.4	340.3
Pd^0 $3d_{5/2}$	335.2	335.1
Pd^{2+} $3d_{3/2}$	342.0	341.7
Pd^{2+} $3d_{5/2}$	336.7	336.4

in the Pd particle size were not reflected in the values of binding energy; they remained almost unchanged for zeolites Pd/HY with the highest Pd loadings (1.5 and 2.5 wt%) – Table 6. However, the confirmation of increasing size of noble metal particles was provided by comprehensive characterization with use of STEM studies (Fig. 10) as well as previously presented results of XRD, low temperature nitrogen sorption and quantitative IR investigations. Consequently, it can be anticipated that the drop in activity

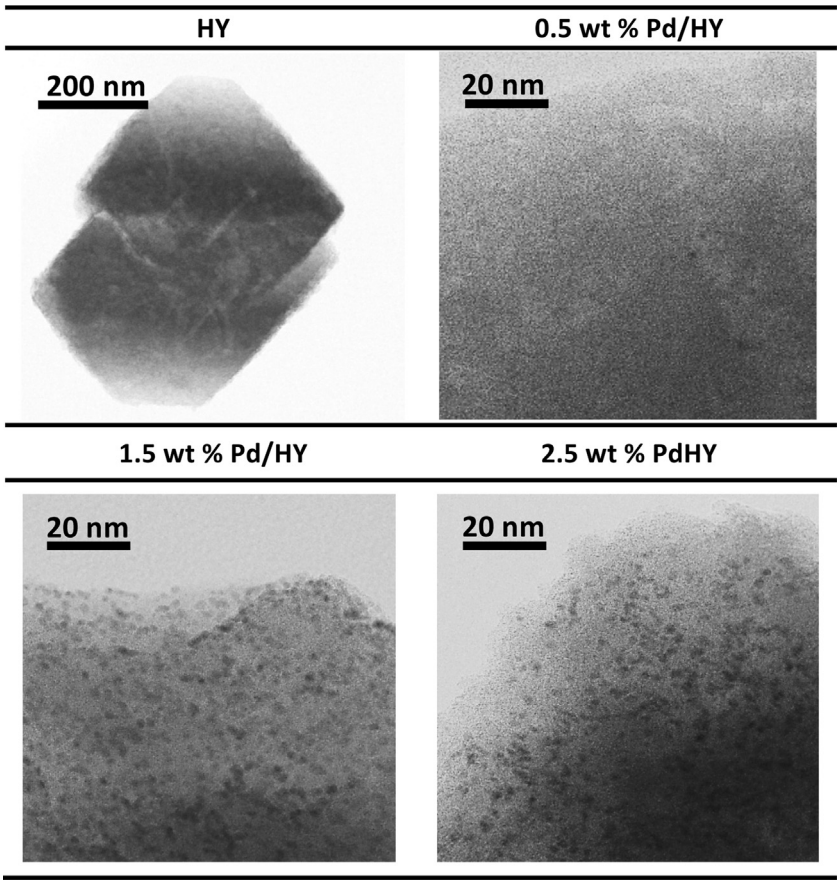

Fig. 10. TEM micrographs of studied zeolites.

observed for zeolite HY with the highest Pd loading (2.5 wt%) can be related to the formation of less dispersed, thus less active forms of Pd species. The plaguing of micropore mouths additionally reduces the role of Brønsted acid sites as the reservoir of substrate chemisorbed.

3.5. On the mechanism of methanol incineration

For the catalysts doped with 1.5 wt% of palladium, which were found to be the most active in each series of the samples turn over frequencies (TON) values were calculated for the reaction performed at 100 °C. It was assumed that each surface Pd species, determined by quantitative pyridine sorption, is an active centre for methanol conversion. The TON values determined for 1.5 wt% Pd/HY, 1.5 wt% Pd/NaY and 1.5 wt% Pd/Al_2O_3 are 37.6, 6.7 and 1.2 s^{-1}, respectively. Such significant differences in activity of the individual Pd-centres are possibly related to the extent of noble metal species aggregation. As it was shown in Fig. 3, the less aggregated Pd-species were present in a series of the Pd/HY samples, which exhibited the best catalytic activity. On the other hand, the lowest catalytic activity was stated for the Pd/Al_2O_3 series, in which noble metal was present in the form of more clustered species. Thus, it could be concluded that highly dispersed palladium species exhibit highly enhanced activity in the process of methanol oxidation in comparison with more aggregated, clustered ones. Another result, which supports, this hypothesis is a decrease in the activity of the catalysts with the highest palladium loading. As it was shown in Fig. 2, an increase in the intended content of noble metal from 1.5 to 2.5 wt%, despite the maintained Pd particles size (Table 1), results in the higher agglomeration degree. It implies the negative effect on catalytic activity by limiting the accessibility of hidden inside micropores active sites, both Brønsted sites and palladium species, to reagent molecules.

Another important issue is the role of palladium species in the catalytic oxidation process. Several reaction mechanisms have been proposed for VOCs oxidation. The surface reaction between two adsorbed species on active sites is postulated as the rate determining step of oxidation reaction in the Langmuir–Hinshelwood (L–H) mechanism, while the reaction between molecule chemisorbed on the catalyst surface with another molecule from the gas phase is recognized as the Eley–Rideal (E–R) mechanism. The mechanism, widely applied for the explanation of organic molecules oxidation, is the Mars-van Krevelen (MVK) oxidative–reductive mechanism involving reaction of reagent molecule and oxygen on different redox sites. The validity of each mechanism strongly depends on type of noble metal, nature of the support as well as on the properties of VOC molecule.

It seems that palladium is the most active in oxidation of methane among noble metals, however its catalytic action depends noticeably on the type of support and reaction conditions. There are different reports concerning the effect of the Pd oxidation state on hydrocarbons catalytic oxidation [54,55]. The mixture of Pd^0 and Pd^{2+} has been considered as the most catalytically active phase: Pd^{2+} is active in hydrocarbons combustion, while the presence of Pd^0 additionally enhances catalytic activity by providing more active sites for VOCs dissociation.

It was shown by XPS studies that in the studied catalysts palladium is deposited both in metallic and oxide forms. The IR studies of methanol, formaldehyde, methane transformation in the absence of gaseous oxygen showed that these molecules can be oxidised by PdO_x species, which during this process are reduced to metallic Pd^0 form. Thus, the MVK pathway seems to be adapted for HCHO,

CH_3OH and CH_4 oxidation. A crucial role, determining activity of the catalysts, plays the redox properties of Pd-aggregates of various sizes. Additionally, Pd particles deposited on acidic supports can be more easily oxidized than those supported on neutral or basic support. The acidic supports of electrophilic properties can result in the electron deficient Pd atoms, thus the facility of Pd^0 to Pd^{2+} oxidation can also enhance the catalytic Mars-van Krevelen (MVK) oxidative–reductive pathway. The Brønsted acid sites are also the additional reservoir of chemisorbed substrate, mainly for methanol and formaldehyde adsorption. In conclusion, the superior catalytic activity of 1.5 wt% Pd/HY is a synergetic effect of a high acidity of the zeolitic support and high Pd dispersion. Reaction mechanism similar to the well-known Mars–van Krevelen mechanism has been reported also for HCHO oxidation over the bimetallic 0.25Pd/20Mn/Beta catalyst [95]. In general the Mars–van Krevelen mechanism is applicable to high-temperature oxidation reactions above 400 °C [96], nevertheless the kinetic synergism between the direct and indirect reaction pathways has been reported to be responsible for lowering the reaction temperature to near room temperature [95].

4. Conclusions

Zeolites (Na/H)Y and Al_2O_3 doped with palladium were found to be active catalysts for low-temperature methanol oxidation to CO_2 and H_2O. In a series of the zeolite catalysts the best results were obtained for palladium deposited on protonic form of zeolite Y (HY), which were more active than the catalysts based on sodium form of zeolite (NaY) and Al_2O_3. The differences in the catalytic performance of these systems were attributed to various aggregation of Pd-species, which determines their activity in the process of methanol incineration. Palladium in the form of well dispersed species was found to be significantly more active than aggregated species of this noble metal. It was suggested that the surface acidity (nature and density of acid sites) of the supports influenced the aggregation of palladium species. The optimal palladium loading, guarantying high catalytic activity in the low-temperature process of methanol incineration, was found to be 1.5 wt%. An increase in the Pd content above this value resulted in a decrease in catalytic activity due to the formation of more clustered palladium aggregates, which partially blocked the zeolite pore system.

Acknowledgments

This work was financed by Grant No. 2013/09/B/ST5/00066 from the National Science Centre, Poland.

The catalytic tests were carried out with the equipment purchased thanks to the financial support of the European Regional Development Fund in the framework of the Polish Innovation Economy Operational Program (contract no. POIG.02.01.00-12-023/08).

The TEM studies were realized within the frame of the project "Infrastructure Improving of Centre of Excellence of Advanced Materials with Nano- and Submicron- Structure", which is supported by the operational Program "Research and Development" financed through European Regional Development Fund.

References

[1] M.J. Molina, Pure Appl. Chem. 68 (1996) 1749–1756.
[2] R. Atkinson, Atmos. Environ. 34 (2000) 2063–2101.
[3] A. Gervasini, G.C. Vezzoli, V. Ragaini, Catal. Today 29 (1996) 449–455.
[4] J.J. Li, X.Y. Xu, Z. Jiang, Z.P. Hao, C. Hu, Environ. Sci. Technol. 39 (2005) 1319–1323.
[5] M. Guillemont, J. Mijoin, S. Mignard, P. Magnoux, Appl. Catal. B: Environ. 75 (2007) 249–255.
[6] K. Narui, K. Furuta, H. Yata, A. Nishida, Y. Kohtoku, T. Matsuzaki, Catal. Today 45 (1998) 173–178.
[7] W. Lin, Y.X. Zhu, N.Z. Wu, Y.C. Xie, I. Murwani, E. Kemnitz, Appl. Catal. B: Environ. 50 (2004) 59–66.
[8] J.-F. Lamonier, A.-B. Boutoundou, C. Gennequin, M.J. Pérez-Zurita, S. Siffert, A. Aboukais, Catal. Lett. 118 (2007) 165–172.
[9] C. Lahousse, A. Bernier, P. Grange, B. Delmon, P. Papaefthimiou, T. Ioannides, X. Verykios, J. Catal. 178 (1998) 214–225.
[10] P. Doggali, Y. Teraoka, P. Mungse, I.K. Shah, S. Rayalu, N. Labhsetwar, J. Mol. Catal. A: Chem. 358 (2012) 23–30.
[11] M.R. Morales, B.P. Barbero, L.E. Cadús, Appl. Catal. B: Environ. 74 (2007) 1–10.
[12] L.Y. Jin, M. He, J.Q. Lu, M.F. Luo, L.B. Gao, J. He, J. Rare Earths 26 (2008) 614–618.
[13] S.M. Saqer, D.I. Kondarides, X.E. Verykios, Top. Catal. 52 (2009) 517–527.
[14] J.Ch.-S. Wu, Z.-A. Lin, F.-M. Tsai, J.-W. Pan, Catal. Today 63 (2000) 419–426.
[15] M.F.M. Zwinkels, S.G. Jörås, P.G. Menon, T.A. Griffin, Catal. Rev. Sci. Eng. 35 (1993) 319–358.
[16] E.M. Cordi, J.L. Falconer, J. Catal. 162 (1996) 104–117.
[17] B. Coq, J.M. Cognion, F. Figueras, D. Tournigant, J. Catal. 141 (1993) 21–33.
[18] A. Morato, C. Alonso, F. Medina, Y. Cesteros, P. Salagre, J.E. Sueiras, D. Tichit, B. Coq, Appl. Catal. B: Environ. 32 (2001) 167–179.
[19] J.C.-S. Wu, Z.-A. Lin, J.-W. Pan, M.-H. Rei, Appl. Catal. A: Gen. 219 (2001) 117–124.
[20] J.R. Gonzàlez-Velasco, A. Aranzabal, J.I. Gutiérrez, R. Lopez-Fonseca, M.A. Gutiérrez-Ortiz, Appl. Catal. B: Environ. 19 (1998) 189–197.
[21] P. Papaefthimiou, T. Ioannides, X.E. Verykios, Appl. Therm. Eng. 18 (1998) 1005–1012.
[22] P. Papaefthimiou, T. Ioannides, X.E. Verykios, Appl. Catal. B: Environ. 13 (1997) 175–184.
[23] K. Nomura, K. Noro, Y. Nakamura, H. Yoshida, A. Satsuma, T. Hattori, Catal. Lett. 58 (1999) 127–130.
[24] W.S. Epling, G.B. Hoflund, J. Catal. 182 (1999) 5–12.
[25] T. Garcia, B. Solsona, D.M. Murphy, K.L. Antcliff, S.H. Taylor, J. Catal. 229 (2005) 1–11.
[26] T. Garcia, B. Solsona, D. Cazorla-Amores, A. Linares-Solano, S.H. Tayor, Appl. Catal. B: Environ. 62 (2006) 66–76.
[27] J.J. Spivey, J.B. Butt, Catal. Today 11 (1992) 465–500.
[28] J. Tsou, P. Magnoux, M. Guisnet, J.J.M. Órfão, J.L. Figueiredo, Appl. Catal. B: Environ. 57 (2005) 117–123.
[29] B. Grbic, N. Radic, A. Terlecki-Baricevic, Appl. Catal. B: Environ. 50 (2004) 161–166.
[30] R.S.G. Ferreira, P.G.P. de Olivera, F.B. Noronha, Appl. Catal. B: Environ. 50 (2004) 243–249.
[31] A.F. Pérez-Cadenas, S. Maorales-Torres, F. Kapteijn, F.J. Maldonado-Hódar, F. Carrasco-Marín, C. Moreno-Castilla, J.A. Moulijn, Appl. Catal. B: Environ. 77 (2008) 272–277.
[32] C.-K. Shi, L.-F. Yang, Z.-C. Wang, X.-E. He, J.-X. Cai, G. Li, X.-S. Wang, Appl. Catal. A: Gen. 243 (2003) 379–388.
[33] H.L. Tidahy, M. Hosseni, S. Siffert, R. Cousin, J.-F. Lamonier, A. Aboukaïs, B.-L. Su, J.-M. Giraudon, G. Leclercq, Catal. Today 137 (2008) 335–339.
[34] H.L. Tidahy, S. Siffert, F. Wyrwalski, J.-F. Lamonier, A. Aboukaïs, Catal. Today 119 (2007) 317–320.
[35] H.L. Tidahy, S. Siffert, J.-F. Lamonier, E.A. Zhilinskaya, A. Aboukaïs, Z.-Y. Yuan, A. Vantomme, B.-L. Su, X. Canet, G. De Weireld, M. Frère, T.B. N'Guyen, J.-M. Giraudon, G. Leclercq, Appl. Catal. A: Gen. 310 (2006) 61–69.
[36] J. Carpentier, J.F. Lamonier, S. Siffert, E.A. Zhilinskaya, A. Aboukaïs, Appl. Catal. A: Gen. 234 (2002) 91–101.
[37] F.X. Yin, S.F. Ji, P.Y. Wu, F.Z. Zhao, C.Y. Li, J. Catal. 257 (2008) 108–116.
[38] W.G. Shim, J.W. Lee, S.C. Kim, Appl. Catal. B: Environ. 84 (2008) 133–141.
[39] K. Okumura, T. Kobayashi, H. Tanaka, M. Niwa, Appl. Catal. B: Environ. 44 (2003) 325–331.
[40] J.J. Li, Z. Jiang, Z.P. Hao, X.Y. Xu, Y.H. Zhuang, J. Mol. Catal. A: Chem. 225 (2005) 173–179.
[41] L.S. Feio, J.C. Escritori, F.B. Noronha, C.E. Hori, Catt. Lett. 120 (2008) 229–235.
[42] S.C. Kim, W.G. Shim, Appl. Catal. B: Environ. 92 (2009) 429–436.
[43] S.K. Ihm, Y.D. Jun, D.C. Kim, K.E. Jeong, Catal. Today 93–95 (2004) 149–154.
[44] P. Dege, L. Pinard, P. Magnoux, M. Guisnet, Appl. Catal. B: Environ. 27 (2000) 17–26.
[45] S. Huang, C. Zhang, H. He, Catal. Today 139 (2008) 15–23.
[46] Y. Yazawa, H. Yoshida, N. Takgi, S. Komai, A. Sutsuma, T. Hattori, Appl. Catal. B: Environ. 19 (1996) 261–266.
[47] R. Burch, P.K. Loader, F.J. Urbano, Catal. Today 27 (1996) 243–248.
[48] R.J. Farrauto, M.C. Hobson, T. Kennelly, E.M. Waterman, Appl. Catal. A: Gen. 81 (1992) 227–237.
[49] C.A. Muller, M. Maciejewski, R.A. Koeppel, A. Baiker, J. Catal. 166 (1997) 36–43.
[50] P.O. Thevenin, E. Pocoroba, L.J. Pettersson, H. Karhu, I.J. Vayrynen, S.G. Jaras, J. Catal. 207 (2002) 139–149.
[51] K. Okumura, S. Matsumoto, N. Nishiaki, M. Niwa, Appl. Catal. B: Environ. 40 (2003) 151–159.
[52] J.N. Carstens, S.C. Su, A.T. Bell, J. Catal. 176 (1998) 136–142.
[53] M. Lyubovsky, L. Pfefferle, Appl. Catal. A: Gen. 173 (1998) 107–119.
[54] M. Lyubovsky, L. Pfefferle, Catal. Today 47 (1999) 29–44.
[55] Ch. He, J. Li, P. Li, J. Cheng, Z. Hao, Z.-P. Xu, Appl. Catal. B: Environ. 96 (2010) 466–475.
[56] J. Bedia, J.M. Rosasa, J. Rodríguez-Mirasol, T. Cordero, Appl. Catal. B: Environ. 94 (2010) 8–18.
[57] L.F. Liotta, Appl. Catal. B: Environ. 100 (2010) 403–412.
[58] K. Muto, N. Katada, M. Niwa, Appl. Catal. B: Environ. 134 (1996) 203–215.

[59] Y. Yazawa, H. Yoshida, N. Takagi, S. Komai, A. Satsuma, T. Hattori, J. Catal. 187 (1999) 15–23.
[60] P. Briot, M. Primet, Appl. Catal. A: Gen. 68 (1991) 301–314.
[61] A. Baylet, S. Royer, P. Marecot, J.M. Tatibouet, D. Duprez, Appl. Catal. B: Environ. 81 (2008) 88–96.
[62] R.S.G. Ferreira, P.G.P. de Oliveira, F.B. Noronha, Appl. Catal. B: Environ. 50 (2004) 243–249.
[63] O. Demoulin, G. Rupprechter, I. Seunier, B. Le Clef, M. Navez, P. Ruiz, J. Phys. Chem. B 109 (2005) 20454–20462.
[64] P. Papaefthimiou, T. Ioannides, X.E. Verykios, Appl. Catal. B: Environ. 15 (1998) 75–92.
[65] N. Burgos, M. Paulis, M.M. Antxustegi, M. Montes, Appl. Catal. B: Environ. 38 (2002) 251–258.
[66] D. Delimaris, T. Ionnides, Appl. Catal. B: Environ. 89 (2009) 295–302.
[67] K. Okumura, J. Amano, N. Yasunobu, M. Niwa, J. Phys. Chem. B 104 (2000) 1050–1057.
[68] Ch. He, P. Li, J. Cheng, Z.-P. Hao, Z.-P. Xu, Water Air Soil Pollut. 209 (2010) 365–376.
[69] H.L. Tidahy, S. Siffert, J.-F. Lamonier, R. Cousin, E.A. Zhilinskaya, A. Aboukaïs, B.-L. Su, X. Canet, G. De Weireld, M. Frère, J.-M. Giraudon, G. Leclercq, Appl. Catal. B: Environ. 70 (2007) 377–383.
[70] H.L. Tidahy, S. Siffert, J.-F. Lamonier, E.A. Zhilianskaya, A. Aboukaïs, B.-L. Su, X. Canet, G. Deweireld, M. Frère, J.-M. Gireaudon, G. Leclercq, Stud. Surf. Sci. Catal. 160 (2007) 209–216.
[71] J. Jacquemin, S. Siffert, J.-F. Lamonier, E. Zhilinskaya, A. Aboukaïs, Stud. Surf. Sci. Catal. 142 (2002) 699–706.
[72] K. Okumura, H. Tanaka, M. Niwa, Catal. Lett. 58 (1999) 43–45.
[73] A. Drelinkiewicz, M. Hasik, M. Kloc, J. Catal. 186 (1999) 123–133.
[74] A. Drelinkiewicz, M. Hasik, S. Quillard, C. Paluszkiewicz, J. Mol. Struct. 511–512 (1999) 205–215.
[75] M. Hasik, A. Bernasik, A. Drelinkiewicz, K. Kowalski, E. Wenda, J. Camra, Surf. Sci. 507–510 (2002) 916–921.
[76] J. Rouquerol, P. Llewellyn, F. Rouquerol, Stud. Surf. Sci. Catal. 160 (2007) 49–56.
[77] K. Sadowska, K. Góra-Marek, J. Datka, Vibr. Spec. 63 (2012) 418–425.
[78] J. Huang, C.J. Xue, B.F. Wang, X.Z. Guo, S.R. Wang, React. Kinet. Mech. Catal. 108 (2) (2013) 403–416.
[79] H.Y. Zhang, B. Dai, X.G. Wang, L.L. Xu, M.Y. Zhu, J. Ind. Eng. Chem. 18 (2012) 49–54.
[80] E.P. Parry, J. Catal. 2 (1963) 371–379.
[81] J. Bellamy, Infrared Spectra of Complex Molecules, second ed., Chapman and Hall, London/New York, 1980.
[82] S. Song, S. Jiang, Appl. Catal. B: Environ. 117–118 (2012) 346–350.
[83] E. Ivanova, M. Mihaylov, F. Thibault-Starzyk, M. Daturi, K. Hadjiivanov, J. Mol. Catal. A 274 (2007) 179–184.
[84] C.M. Piqueras, I.O. Costilla, P.G. Belelli, N.J. Castellani, D.E. Damiani, Appl. Catal. A: Gen. 347 (2008) 1–10.
[85] J. Szanyi, W.K. Kuhn, D.W. Goodman, J. Vac. Sci. Technol. A 11 (4) (1993) 1969–1974.
[86] K. Okumura, M. Niwa, Catal. Surv. Jpn. 5 (2002) 121–126.
[87] R.F. Hicks, H. Qi, M.L. Young, R.G. Lee, J. Catal. 122 (1990) 280–294.
[88] A.P.J. Jansen, R. van Santen, J. Phys. Chem. 94 (1990) 6764–6772.
[89] W.M.H. Sachtler, A.Y. Stakheev, Catal. Today 12 (1992) 283–295.
[90] B.L. Mojet, M.J. Kappers, J.C. Muijsers, J.W. Niemantsverdriet, J.T. Miller, F.S. Modica, D.C. Koningsberger, Stud. Surf. Sci. Catal. 84B (1994) 909–916.
[91] S. Doniacht, M. Sunjic, J. Phys. C Solid State Phys. 3 (1970) 285–291.
[92] K.S. Kim, A.F. Gossmann, N. Winograd, Anal. Chem. 46 (1975) 197–200.
[93] L.S. Kibis, A.I. Titkov, A.I. Stadnichenko, S.V. Koscheev, A.I. Boronin, Appl. Surf. Sci. 255 (2009) 248–9254.
[94] L.V. Nosova, M.V. Stenin, Yu.N. Nogin, Yu.A. Ryndin, Appl. Surf. Sci. 55 (1992) 43–48.
[95] S.J. Park, I. Bae, I.-S. Nama, B.K. Cho, S.M. Jung, J.-H. Lee, Chem. Eng. J. 195–196 (2012) 392–402.
[96] E. Cordi, J. Falconer, J. Catal. 162 (1996) 104–117.